Computer Assisted Mechanics and Engineering Sciences, 8: 567–577, 2001.

Imperfection-sensitivity analysis by using classical and catastrophe theory methods

Marta Kurutz and Zsolt Gáspár
Department of Structural Mechanics, Budapest University of Technology and Economics
Műegyetem rkp. 3, H 1521 Budapest, Hungary

(Received February 21, 2000)

Comparison of the classical methods and the tools of the catastrophe theory is presented through the imperfection-sensitivity analysis of the classical stable-symmetric bifurcation problem. Generally, classical *global* methods are related to a large interval, while catastrophe theory concerns the neighborhood of the critical point only, being a *local* method. Unfortunately, in most cases of practical problems, by using classical global methods, there can hardly be obtained analytical solutions for the multivalued imperfection-sensitivity functions and the associated highly folded imperfection-sensitivity surfaces. In this paper, an approximate solution based on the catastrophe theory is presented, in comparison with the exact solution obtained in graphical way. It will be shown that by considering the problem as an imperfect version (at a fixed imperfection) of a higher order catastrophe, a topologically good solution can be obtained in a considerably large, quasi in a *nonlocal* domain.

1. Introduction

Catastrophe theory in comparison with the classical methods is presented, applied to the imperfection-sensitivity analysis of the classical stable-symmetric bifurcation problem. Imperfection-sensitivity analysis of the three classical types of bifurcation, the stable- and unstable-symmetric and the asymmetric bifurcation, is detailed in [7] related to geometric imperfection and perfectly dead loading devices. However, it may happen in practice that the nature of loading process is not perfectly "dead", namely, it is not perfectly independent of the occurring deflections. On the contrary, some loading devices – for example the hydraulic loading – show certain deformation-sensitive but conservative characteristics leading to the term „configuration-dependent" loading device detailed in [1].

Modification of the classical finite element model in the case of deformation-sensitive loading devices is introduced in [3] by modifying the tangent stiffness of the structure. Comparison of the effect of dead and configuration-dependent loading devices on the postbifurcation behaviour of structures, the modifications of the classical postbifurcation equilibrium paths are detailed in [4]. However, the path dependent characteristics of loading devices can be considered as imperfection of the dead loading program. Imperfection-sensitivity analysis of the three classical bifurcation models with simultaneous material, geometric and loading imperfections is investigated in [5] where the mathematical difficulties of any analytical solutions concerning the imperfection-sensitivity functions are made evident. On the basis of the classical methods, the exact imperfection-sensitivity surfaces can be represented by certain sections only, obtained by graphical way. Even in the simple examples of the well-known basic bifurcation models, the analytical solution of the global analysis can not be performed. Any approximate version restricts the solution to a local domain with doubtful correctness. In this paper, approximate solutions are introduced based on the principles of the catastrophe theory applied to structural stability problems [2, 6]. It will be proved that by considering the problem as an imperfect version of a higher order catastrophe, a topologically good solution can be obtained in a considerably large domain.

2. Classical and loading imperfections

The three classical models of bifurcation with the referring equilibrium paths $\lambda(q)$ are seen in Fig. 1 for one parameter dead load $F = \lambda F_0$ where $F_0 = 1$ is the basic loading level and λ is the loading parameter. In Figs. 1a and 1b the stable and unstable-symmetric, while in Fig. 1c the asymmetric bifurcation model are seen, respectively [7]. These types of simple structural models are assumed to be composed by a perfectly rigid element pinned to a rigid foundation and connected to the support by linear elastic springs.

The classical imperfection-sensitivity functions $\lambda_{cr}(\varepsilon_g)$ are also seen in Fig. 1 related to geometric imperfection ε_g only. The system is *geometrically perfect* in the sense that the springs are unstrained when the links are vertical, that is $\varepsilon_g = 0$.

In this paper the stable-symmetric bifurcation problem is analyzed only, by extending the analysis to loading imperfections, moreover, to the interaction of the geometric and loading type imperfections, as well.

Let us consider F as the given external load acting vertically on the top of the rods in Fig. 1. If the load F is independent of the occurring displacement u, it is a *dead* load, while if it is in interaction with u, it is a *configuration-dependent* load. Fundamental aspects and classification of loading devices are detailed in [1].

Dead type conservative loading device supposes the applied load to be independent of the occurring deflections. This kind of loading process can be characterized by the function $F = \lambda F_0$ regularizing the load level by the scalar parameter λ, seen in Fig. 2c. *Configuration-dependent or deformation-sensitive* conservative loading process assumes the applied load to be dependent on the occurring deflections, but to be path-independent [1]. This kind of loading device can be specified by a load–deflection function $F(u) = \lambda F_0 + f(u)$ containing the classical *controllable* part λF_0 governed

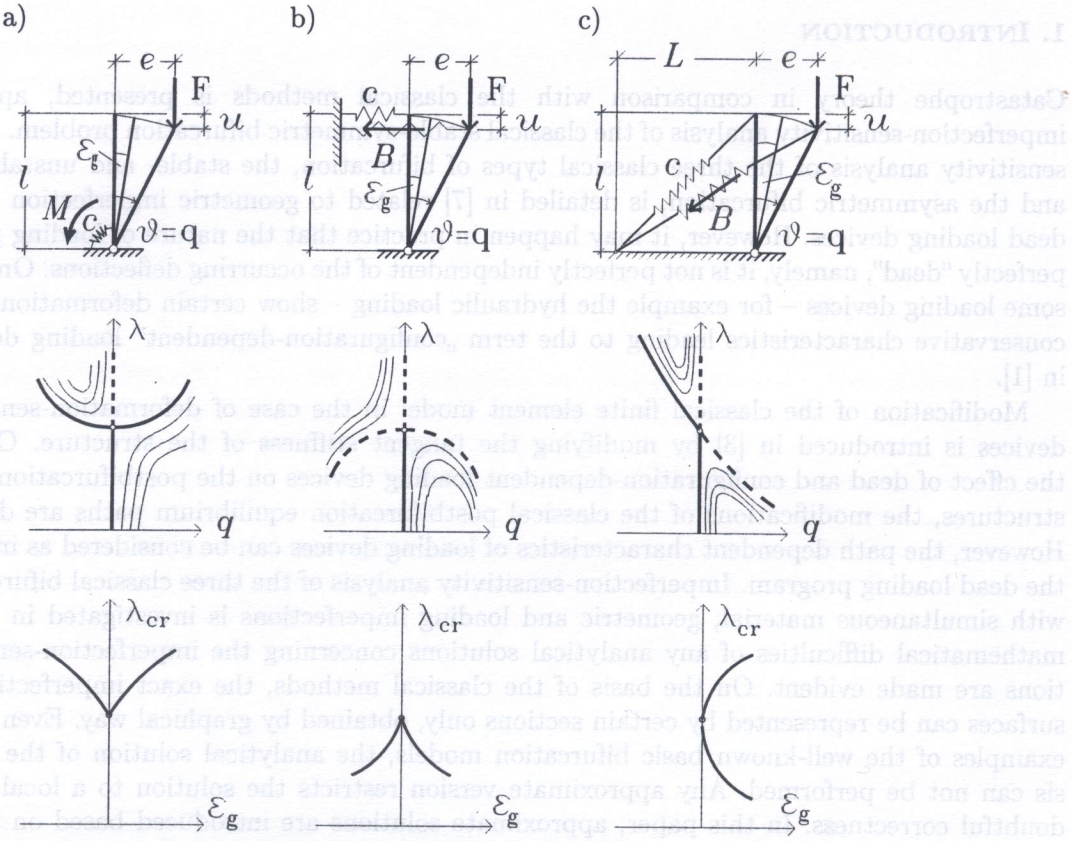

Fig. 1. The three classical bifurcation models, equilibrium paths and the classical imperfection-sensitivity functions; a) stable-symmetric, b) unstable-symmetric, c) asymmetric

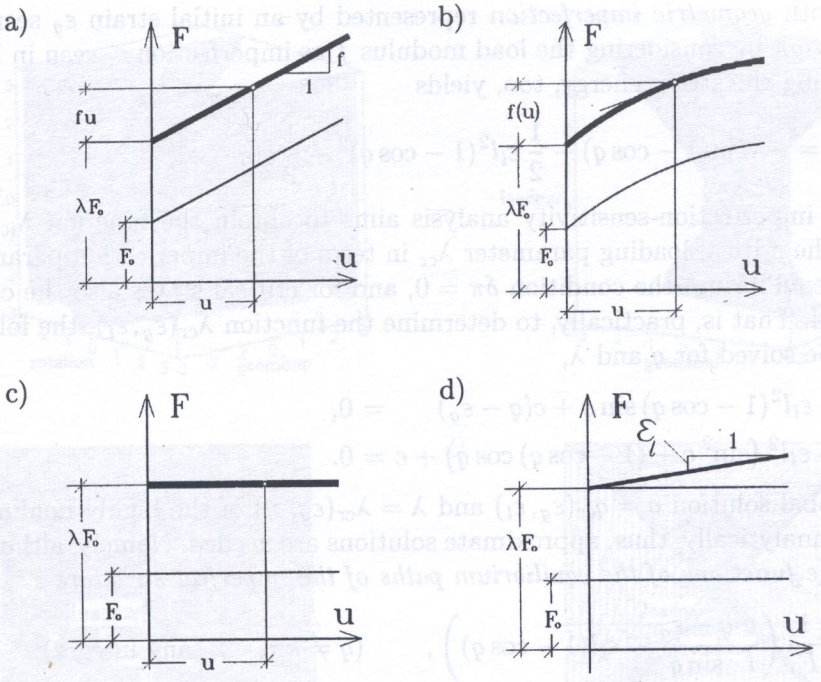

Fig. 2. The configuration-dependent loading and the loading imperfection; a) linear configuration-dependent loading, b) nonlinear configuration-dependent loading, c) dead loading, d) loading imperfection

by the load parameter λ, and the *deformation-sensitive* part $f(u)$ specified as a linear or nonlinear function, seen in Figs. 2a and 2b. For the linear case the function is $F(u) = \lambda F_0 + fu$.

In this paper linear configuration-dependent loading is considered as *loading imperfection*. The system is perfect in the sense that the load is perfectly dead, that is $f = 0$, thus, the loading tangent $f = \varepsilon_l$ can be considered as *loading imperfection*, seen in Fig. 2d.

Let us consider now the modification of the classical imperfection-sensitivity functions in dependence of the imperfection, that is, the deformation-dependence of the loading device.

In spite of the fact that imperfections are generally small in the classical imperfection-sensitivity analyses, in this study large imperfections are also considered. Namely, the aim of the analysis is to extend the local characteristics of the catastrophe theory to quasi-global one.

3. Geometric-loading imperfection-sensitivity of the stable-symmetric bifurcation model obtained by classical analysis

The linear elastic behaviour of the hinged rod seen in Fig. 1a can be characterized by the stress–strain relation $M = c\vartheta$ where c is the spring constant, M is the moment in the spring and $\vartheta = q$ is the angle of rotation of the rod, representing the strain in the spring. By considering exact nonlinear geometry, the strain–displacement relation is represented by the trigonometric function $u = l(1 - \cos q)$.

In the case of configuration-dependent conservative loading, by assuming the linear function $F(u) = \lambda F_0 + fu$, the external potential yields

$$\pi_{\text{ext}}(q, \lambda) = -\int_u F(u)\,\mathrm{d}u = -\int_u (\lambda F_0 + fu)\,\mathrm{d}u = -\lambda F_0 u - \frac{1}{2} f u^2$$
$$= -\lambda F_0 l(1 - \cos q) - \frac{1}{2} f l^2 (1 - \cos q)^2. \tag{1}$$

In the case of both *geometric imperfection* represented by an initial strain ε_g seen in Fig. 1a, and *loading imperfection* by considering the load modulus f as imperfection ε_l seen in Fig. 2d, the total potential, including the strain energy, too, yields

$$\pi(q, \lambda, \varepsilon_g, \varepsilon_l) = -\lambda F_0 l(1 - \cos q) - \frac{1}{2}\varepsilon_l l^2 (1 - \cos q)^2 + \frac{1}{2} c(q - \varepsilon_g)^2. \tag{2}$$

The classical imperfection-sensitivity analysis aims to obtain the function $\lambda_{icr}(\varepsilon_g, \varepsilon_l)$, namely, the function of the critical loading parameter λ_{cr} in term of the imperfection parameters ε_g , ε_l . As it is known, for equilibrium the condition $\delta\pi = 0$, and for critical states also the condition $\delta^2\pi = 0$ has to be fulfilled. That is, practically, to determine the function $\lambda_{cr}(\varepsilon_g, \varepsilon_l)$, the following system of equations is to be solved for q and λ,

$$-\lambda F_0 l \sin q - \varepsilon_l l^2 (1 - \cos q) \sin q + c(q - \varepsilon_g) \quad = 0, \tag{3}$$

$$-\lambda F_0 l \cos q - \varepsilon_l l^2 \left(\sin^2 q + (1 - \cos q)\cos q\right) + c = 0. \tag{4}$$

However, the global solution $q = q_{cr}(\varepsilon_g, \varepsilon_l)$ and $\lambda = \lambda_{cr}(\varepsilon_g, \varepsilon_l)$ of the highly nonlinear problem can not be obtained analytically, thus, approximate solutions are needed. Namely, although from Eq. (3) we can obtain *the functions of the equilibrium paths of the imperfect structure*

$$\lambda(q, \varepsilon_g, \varepsilon_l) = \frac{1}{F_0}\left(\frac{c}{l}\frac{q - \varepsilon_g}{\sin q} - \varepsilon_l l(1 - \cos q)\right), \qquad (q \neq k\pi, \quad k \text{ any integer}) \tag{5}$$

which can be introduced into Eq. (4) *yielding the function of the tangent stiffness of the imperfect structure* which is vanishing at the critical point, namely

$$K(q, \varepsilon_g, \varepsilon_l) = c\left(1 - \frac{q - \varepsilon_g}{tgq}\right) - \varepsilon_l l^2 \sin^2 q = 0, \qquad (q \neq k\pi), \tag{6}$$

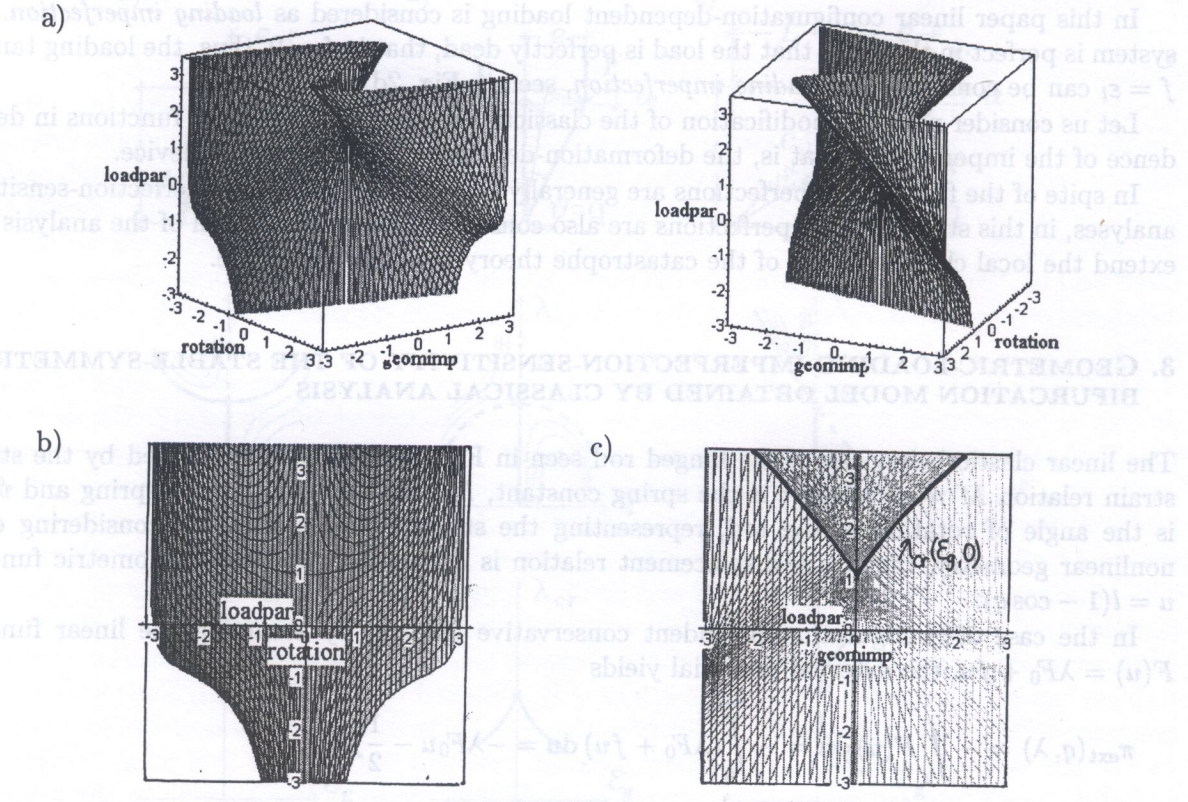

Fig. 3. Geometric imperfection-sensitivity; a) equilibrium surface $\lambda(q, \varepsilon_g, 0)$, b) sections of $\lambda(q, \varepsilon_g, 0)$ for constant ε_g , c) section $\lambda_{cr}(\varepsilon_g, 0)$ of the imperfection-sensitivity surface $\lambda_{cr}(\varepsilon_g, \varepsilon_l)$

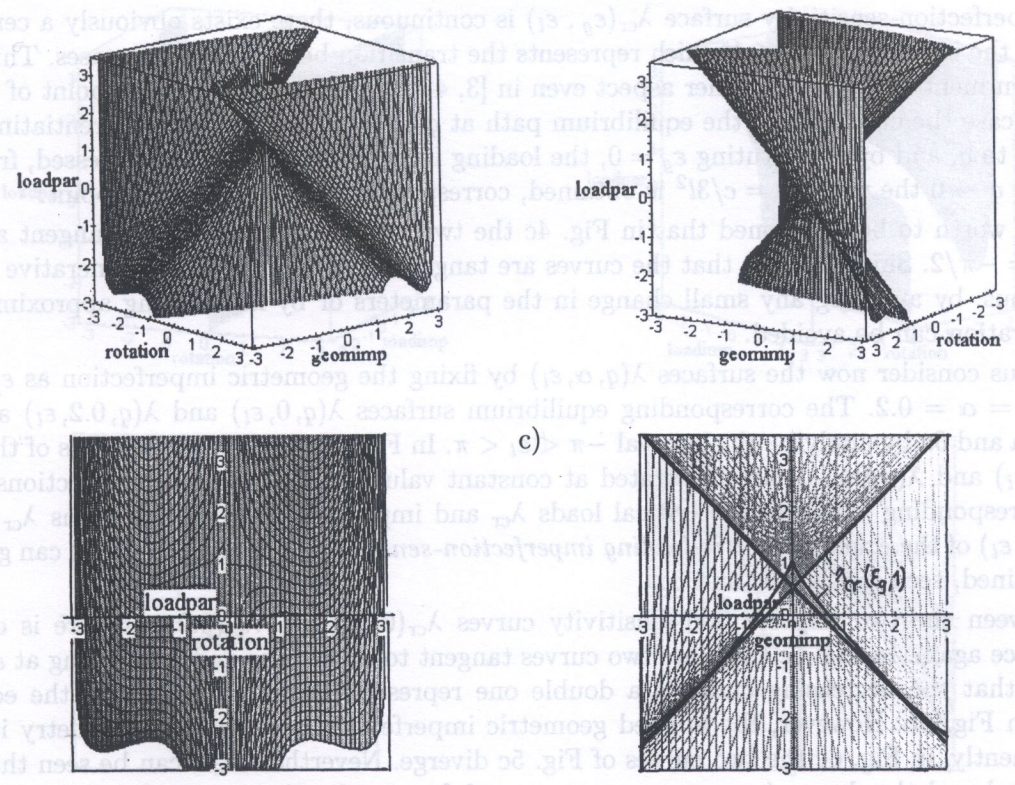

Fig. 4. Geometric imperfection-sensitivity influenced by loading imperfection; a) equilibrium surface $\lambda(q, \varepsilon_g, 1)$, b) sections of $\lambda(q, \varepsilon_g, 1)$ for constant ε_g, c) section $\lambda_{cr}(\varepsilon_g, 1)$ of the imperfection-sensitivity surface $\lambda_{cr}(\varepsilon_g, \varepsilon_l)$

nevertheless, no analytical solution of this equation exists. Unfortunately, by applying Taylor expansion for the trigonometric functions, the validity of the approximate solution of the imperfection-sensitivity function $\lambda_{cr}(\varepsilon_g, \varepsilon_l)$ will be limited to a local domain of the possible deflections q.

Global solutions can be obtained in a graphical way, only for sections of the imperfection-sensitivity surface $\lambda_{cr}(\varepsilon_g, \varepsilon_l)$, by fixing one of the parameters ε_g and ε_l. For this solution, the equilibrium surface (5) of the imperfect structure is used. The expression $\lambda(q, \varepsilon_g, \varepsilon_l)$ represents a hypersurface, thus, by fixing each of the imperfections as $\varepsilon_g = \alpha$, or $\varepsilon_l = \beta$, the subdomains of $\lambda(q, \varepsilon_g, \varepsilon_l)$, namely, the surfaces $\lambda(q, \alpha, \varepsilon_l)$ or $\lambda(q, \varepsilon_g, \beta)$ can graphically be obtained, from which the critical loads λ_{cr} and critical deflections q_{cr} can be identified. In this way, from the corresponding values of λ_{cr} and ε_g or ε_l, the sections of the *exact imperfection-sensitivity surface* $\lambda_{cr}(\varepsilon_g, \varepsilon_l)$ can graphically be obtained.

In the following, for the numerical examples the values $c = 1$, $l = 1$ and $F_0 = 1$ will be applied. Let us fix first the loading imperfection for the surface $\lambda(q, \varepsilon_g, \beta)$. Two cases are considered: $\varepsilon_l = \beta = 0$ and $\varepsilon_l = \beta = 1$. The corresponding equilibrium surfaces $\lambda(q, \varepsilon_g, 0)$ and $\lambda(q, \varepsilon_g, 1)$ are seen in Figs. 3a and 4a for the intervals $-\pi < q < \pi$ and $-\pi < \varepsilon_g < \pi$. In Figs. 3b and 4b the sections of the surfaces $\lambda(q, \varepsilon_g, 0)$ and $\lambda(q, \varepsilon_g, 1)$ are plotted at constant values for the geometric imperfections ε_g. From the corresponding values of the critical loads λ_{cr} and imperfections ε_g, the sections $\lambda_{cr}(\varepsilon_g, 0)$ and $\lambda_{cr}(\varepsilon_g, 1)$ of the *exact geometric–loading imperfection–sensitivity function* $\lambda_{cr}(\varepsilon_g, \varepsilon_l)$ can graphically be obtained, seen in Figs. 3c and 4c.

The two imperfection-sensitivity curves $\lambda_{cr}(\varepsilon_g, 0)$ and $\lambda_{cr}(\varepsilon_g, 1)$ are qualitatively different. In the case of $\lambda_{cr}(\varepsilon_g, 0)$ in Fig. 3c, there is only a single critical load parameter for each value of ε_g, while for $\lambda_{cr}(\varepsilon_g, 1)$ in Fig. 4c, three of them exist. The reason for this fact is that the geometrically perfect structure exhibits a stable-symmetric bifurcation for the first, and an unstable-symmetric bifurcation for the second case, as it can be seen in Figs. 3b and 4b respectively. Moreover, since

the imperfection-sensitivity surface $\lambda_{cr}(\varepsilon_g, \varepsilon_l)$ is continuous, there exists obviously a certain value of ε_l in the interval $0 \leq \varepsilon_l \leq 1$ which represents the transition between the two cases. This question has been mentioned from another aspect even in [3, 4, 5]. Let us determine the point of transition. In this case the curvature of the equilibrium path at $q = 0$ is zero, thus, by differentiating (6) with respect to q, and by substituting $\varepsilon_g = 0$, the loading imperfection ε_l can be expressed, from which, in limit $q \to 0$ the value $\varepsilon_l = c/3l^2$ is obtained, corresponding to the transition point.

It is worth to be mentioned that in Fig. 4c the two curves have a common tangent at $q = \pi/2$ and $q = -\pi/2$. Since the fact that the curves are tangent to each other is a degenerative characteristic, thus, by applying any small change in the parameters or by introducing approximation, the degeneration can be avoided.

Let us consider now the surfaces $\lambda(q, \alpha, \varepsilon_l)$ by fixing the geometric imperfection as $\varepsilon_g = \alpha = 0$ and $\varepsilon_g = \alpha = 0.2$. The corresponding equilibrium surfaces $\lambda(q, 0, \varepsilon_l)$ and $\lambda(q, 0.2, \varepsilon_l)$ are seen in Figs. 5a and 6a by applying the interval $-\pi < \varepsilon_l < \pi$. In Figs. 5b and 6b the sections of the surfaces $\lambda(q, 0, \varepsilon_l)$ and $\lambda(q, 0.2, \varepsilon_l)$ are illustrated at constant values of the loading imperfections ε_l. From the corresponding values of the critical loads λ_{cr} and imperfections ε_l, the sections $\lambda_{cr}(0, \varepsilon_l)$ and $\lambda_{cr}(0.2, \varepsilon_l)$ of the *exact geometric-loading imperfection-sensitivity function* $\lambda_{cr}(\varepsilon_g, \varepsilon_l)$ can graphically be obtained, seen in Figs. 5c and 6c.

Between the two imperfection-sensitivity curves $\lambda_{cr}(0, \varepsilon_l)$ and $\lambda_{cr}(0.2, \varepsilon_l)$ there is qualitative difference again. In Fig. 5c there are two curves tangent to each other and bifurcating at $\varepsilon_l = c/3l^2$. Notice that the decreasing curve is a double one representing the symmetry of the equilibrium paths in Fig. 5b. However, the applied geometric imperfection destroys the symmetry in Fig. 6b, consequently, in Fig. 6c the two curves of Fig. 5c diverge. Nevertheless, it can be seen that not the horizontal and the decreasing curves are separated from each other, on the contrary, each of the two covering parts of the double curve has been joined with the left or right part of the horizontal curve.

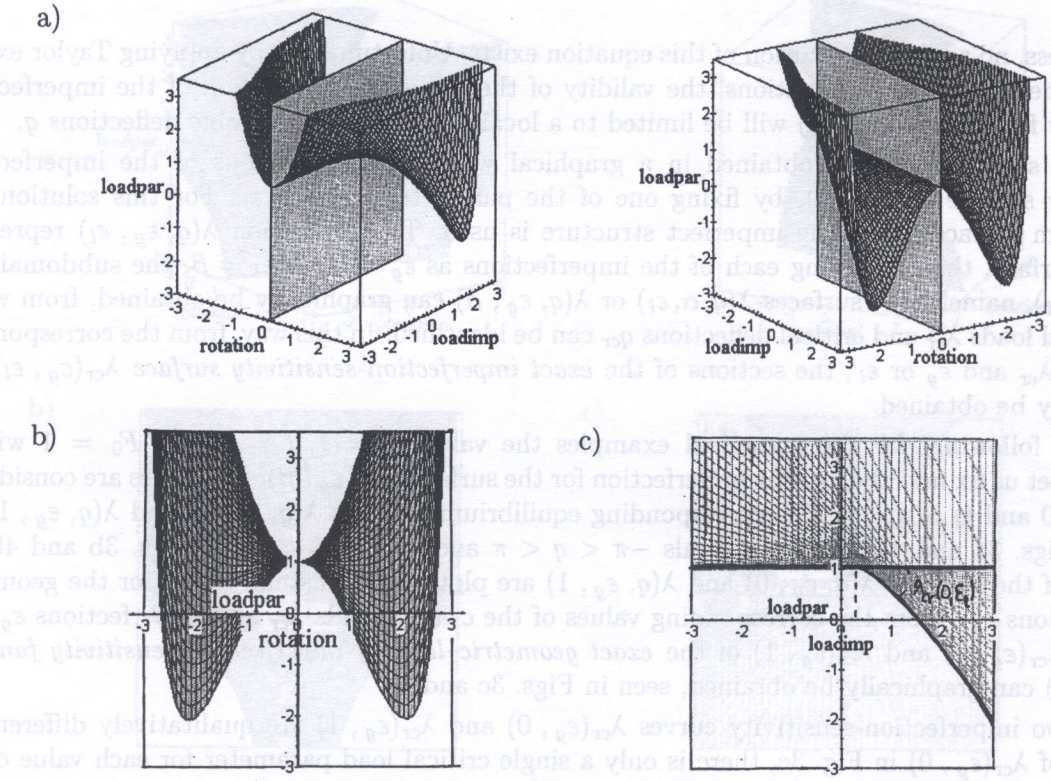

Fig. 5. Loading imperfection-sensitivity; a) equilibrium surface $\lambda(q, 0, \varepsilon_l)$, b) sections of $\lambda(q, 0, \varepsilon_l)$ for constant ε_l, c) section $\lambda_{cr}(0, \varepsilon_l)$ of the imperfection-sensitivity surface $\lambda_{cr}(\varepsilon_g, \varepsilon_l)$

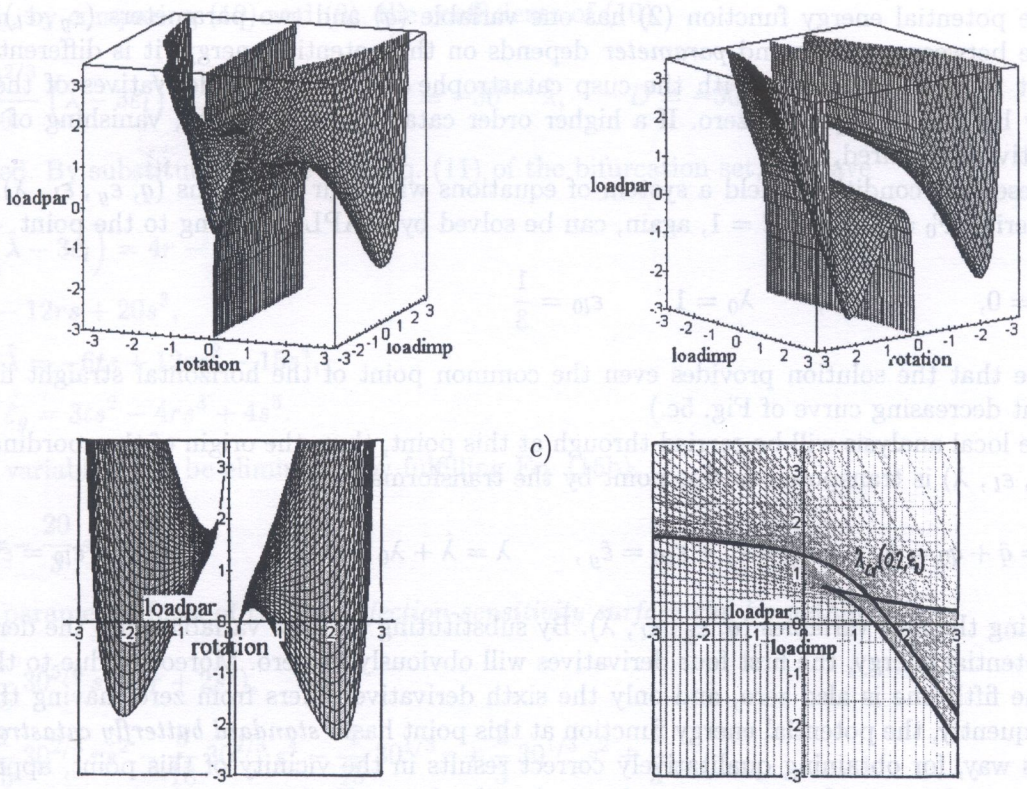

Fig. 6. Loading imperfection-sensitivity influenced by geometric imperfection; a) equilibrium surface $\lambda(q, 0.2, \varepsilon_l)$, b) sections of $\lambda(q, 0.2, \varepsilon_l)$ for constant ε_l, c) section $\lambda_{\mathrm{cr}}(0.2, \varepsilon_l)$ of the imperfection-sensitivity surface $\lambda_{\mathrm{cr}}(\varepsilon_g, \varepsilon_l)$

Notice that in Figs. 5c and 6c the fact can be confirmed again that to smaller values of ε_l a single imperfection-sensitivity point belongs, while to larger values of it three points belong, as we have seen in Figs. 3c and 4c, too. This is obvious since all the curves $\lambda_{\mathrm{cr}}(\varepsilon_g, 0)$ or $\lambda_{\mathrm{cr}}(\varepsilon_g, 1)$ and $\lambda_{\mathrm{cr}}(0, \varepsilon_l)$ or $\lambda_{\mathrm{cr}}(0.2, \varepsilon_l)$ are sections of the same folded surface $\lambda_{\mathrm{cr}}(\varepsilon_g, \varepsilon_l)$.

As for the classical method to obtain the global imperfection-sensitivity function and surface, we can conclude that for the exact global solution, a graphical method can be used, leading to sections of the imperfection-sensitivity surface. Numerically, due to the Taylor expansion of the functions, any solutions are limited to local parts of the global domain.

Let us consider now, how can we solve the problem by using the catastrophe theory. The idea of applying the catastrophe theory is obvious, since it concerns approximate solutions only. As a by-product, the classification of the problem with respect to the types of catastrophes will also be obtained.

4. Geometric-loading imperfection-sensitivity of the stable-symmetric bifurcation model obtained by catastrophe theory

It is known in the catastrophe theory that if an universal unfolding of a catastrophe needs k number of parameters, than in an arbitrarily small vicinity of it all the types of catastrophes occur which need less than k parameters.

It is known [8] that stable-symmetric bifurcation occurs if the total potential energy of the structure has a *standard cusp catastrophe*, while for unstable-symmetric bifurcation a *dual cusp catastrophe* is needed. As we have seen above, in the imperfection domain to be analyzed both cases occur, thus, a higher order than cusp catastrophe is needed, and the local analysis suggested by the catastrophe theory will be investigated at this point.

The potential energy function (2) has one variable (q) and two parameters (ε_g, ε_l). (The difference between *variable* and *parameter* depends on the potential energy: it is differentiated with respect to variables only.) With the cusp catastrophe the first three derivatives of the potential energy have to be equal to zero. If a higher order catastrophe is needed, vanishing of the fourth derivative is required, too.

These four conditions yield a system of equations with four unknowns (q, ε_g, ε_l, λ) which, by considering $F_0 = 1$, $c = 1$, $l = 1$, again, can be solved by MAPLE, leading to the point

$$q_0 = 0, \qquad \varepsilon_{g0} = 0, \qquad \lambda_0 = 1, \qquad \varepsilon_{l0} = \frac{1}{3} \tag{7}$$

(Notice that the solution provides even the common point of the horizontal straight line and its tangent decreasing curve of Fig. 5c.)

The local analysis will be carried through at this point, thus, the origin of the coordinate system (q, ε_g, ε_l, λ) is transposed to this point by the transformations

$$q = \hat{q} + q_0 = \hat{q}, \qquad \varepsilon_g = \hat{\varepsilon}_g + \varepsilon_{g0} = \hat{\varepsilon}_g, \qquad \lambda = \hat{\lambda} + \lambda_0 = \hat{\lambda} + 1, \qquad \varepsilon_l = \hat{\varepsilon}_l + \varepsilon_{l0} = \hat{\varepsilon}_l + \frac{1}{3}, \tag{8}$$

obtaining the new variables ($\hat{q}$, $\hat{\varepsilon}_g$, $\hat{\varepsilon}_l$, $\hat{\lambda}$). By substituting the new variables into the derivatives of the potential energy, the first four derivatives will obviously be zero. Moreover, due to the symmetry, the fifth one is also zero, and only the sixth derivative differs from zero, having the value 4. Consequently, the potential energy function at this point has *a standard butterfly catastrophe* point. In this way, for obtaining qualitatively correct results in the vicinity of this point, approximating the potential energy function up to the sixth order by its Taylor-expansion seems to be enough. Since the coefficient of the sixth order term of the Taylor-expansion is nonzero even at the origin, the effect of the imperfections in the coefficient of the sixth order term can be neglected. But the coefficients of the lower order terms are zero at the origin, so the effect of the imperfections in these terms are to be considered,

$$\pi\left(q, \hat{\varepsilon}_g, \hat{\lambda}, \hat{\varepsilon}_l\right) = \frac{1}{180}q^6 + \frac{1}{24}q^4\left(\hat{\lambda} - 3\hat{\varepsilon}_l\right) - \frac{1}{2}q^2\hat{\lambda} - q\hat{\varepsilon}_g. \tag{9}$$

The canonical form of the butterfly catastrophe

$$f(x, A, B, C, D) = \frac{1}{6}x^6 + \frac{A}{4}x^4 + \frac{B}{3}x^3 + \frac{C}{2}x^2 + Dx \tag{10}$$

has been analyzed intensively in [6] concluding that the points of its bifurcation set can be described by means of the parameters r, s, t seen in [2] as

$$A = 4r - 10s^2, \tag{11a}$$

$$B = 3t - 12rs + 20s^3, \tag{11b}$$

$$C = -6ts + 12rs^2 - 15s^4, \tag{11c}$$

$$D = 3ts^2 - 4rs^3 + 4s^5. \tag{11d}$$

To use these parameters, function (9) has to be derived from the canonical form (10). By applying the transformation

$$x = 30^{1/6}q, \tag{12}$$

the form can be obtained

$$\pi(x, \hat{\varepsilon}_g, \hat{\lambda}, \hat{\varepsilon}_l) = \frac{1}{6}x^6 + \frac{30^{2/3}}{24}x^4\left(\hat{\lambda} - 3\hat{\varepsilon}_l\right) - \frac{30^{1/3}}{2}x^2\hat{\lambda} - 30^{1/6}x\hat{\varepsilon}_g, \tag{13}$$

from which, by comparing (10) and (9), the coefficients of (10)

$$A = \frac{30^{2/3}}{6}\left(\hat{\lambda} - 3\hat{\varepsilon}_l\right), \qquad B = 0, \qquad C = -30^{1/3}\,\hat{\lambda}, \qquad D = -30^{1/6}\,\hat{\varepsilon}_g, \tag{14}$$

are obtained. By substituting these into Eq. (11) of the bifurcation set, we have

$$\frac{30^{2/3}}{6}\left(\hat{\lambda} - 3\hat{\varepsilon}_l\right) = 4r - 10s^2, \tag{15a}$$

$$0 = 3t - 12rs + 20s^3, \tag{15b}$$

$$-30^{1/3}\,\hat{\lambda} = -6ts + 12rs^2 - 15s^4, \tag{15c}$$

$$-30^{1/6}\,\hat{\varepsilon}_g = 3ts^2 - 4rs^3 + 4s^5. \tag{15d}$$

where the variable t can be eliminated by fulfilling Eq. (15b),

$$t = 4rs - \frac{20}{3}s^3. \tag{16}$$

Thus, the parametric form of the *imperfection-sensitivity surface* can be obtained,

$$\varepsilon_g = \frac{4}{15}30^{5/6}\,s^3(-r + 2s^2), \tag{17a}$$

$$\varepsilon_l = \frac{2}{15}30^{2/3}\,rs^2 - \frac{5}{18}30^{2/3}\,s^4 - \frac{4}{15}30^{1/3}\,r + \frac{2}{3}30^{1/3}\,s^2 + \frac{1}{3}, \tag{17b}$$

$$\lambda = -\frac{1}{30}s^2(-12r + 25s^2)30^{2/3} + 1, \tag{17c}$$

as a section of the bifurcation set. By means of the above expressions, the approximate versions of the classical imperfection-sensitivity curves can be calculated on the basis of the catastrophe theory.

Figures 3c and 4c illustrate the sections of the imperfection-sensitivity surface at $\varepsilon_l = 0$ and $\varepsilon_l = 1$, respectively. In both cases, from Eq. (17b) parameter r can be expressed in term of s. By substituting this into Eqs. (17a) and (17c), the required sections of the imperfection-sensitivity surface can be obtained, seen in Figs. 7a and 7b. By comparing Figs. 3c and 4c with Figs. 7a and 7b, respectively, the correspondence between the exact and the approximate curves seems to be evident. In the second case the curves do not tangent each other any more due to the approximation.

Figures 5c and 6c illustrate the sections of the imperfection-sensitivity surface at $\varepsilon_g = 0$ and $\varepsilon_g = 0.2$, respectively. In the first case, from the first equation of (17) two solutions are obtained: $s = 0$ and r is arbitrary, or $r = 2s^2$. By substituting the first solution into the other two equations of (17), the horizontal line $\lambda = 1$ and its decreasing tangent curve are obtained, seen in Fig. 8a. Naturally, this latter is a double curve again, since to any values $+s$ and $-s$ the same point belongs.

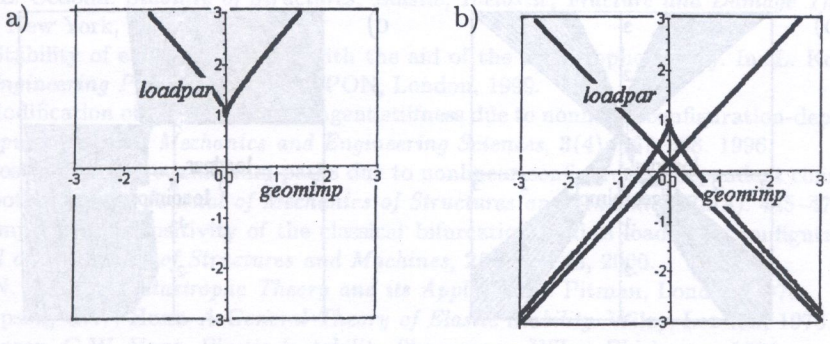

Fig. 7. Sections of imperfection-sensitivity surface $\lambda_{cr}(\varepsilon_g\,,\,\varepsilon_l)$ obtained by catastrophe theory; a) section $\lambda_{cr}(\varepsilon_g\,,\,0)$, b) section $\lambda_{cr}(\varepsilon_g\,,\,1)$

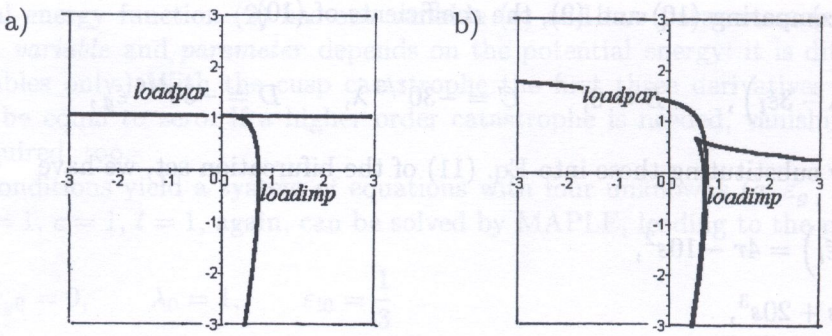

Fig. 8. Sections of imperfection-sensitivity surface $\lambda_{cr}(\varepsilon_g\,,\,\varepsilon_l)$ obtained by catastrophe theory; a) section $\lambda_{cr}(0,\varepsilon_l)$, b) section $\lambda_{cr}(0.2,\varepsilon_l)$

In the second case, value of r can be expressed unambiguously. Although in this expression the denominator is zero at $s = 0$, even this condition separates the two curves seen in Fig. 8b. By comparing Figs. 5c and 6c with Figs. 8a and 8b, respectively, the conclusion is the same in this case, too: the approximation provides topologically equal solution to the exact one. Namely, the topologically equal figures contain the same features of curves: a smooth and a cusped one. Moreover, for $\varepsilon_g = 0$ (Figs. 5c and 8a) the two curves partly coincide, while for $\varepsilon_g = 0.2$ (Figs. 6c and 8b) they are separated. However, in spite of topologic equality, the associated curves are different in geometry.

Moreover, the catastrophe theory solution provides the visualisation of the whole imperfection-sensitivity surface, too. Since it is expressed in parametric form (17), it can be illustrated in three dimensions, as seen in Fig. 9. Although the surface can not be expressed in term of the imperfections being multivalued, by using the catastrophe theory, the visualisation is possible.

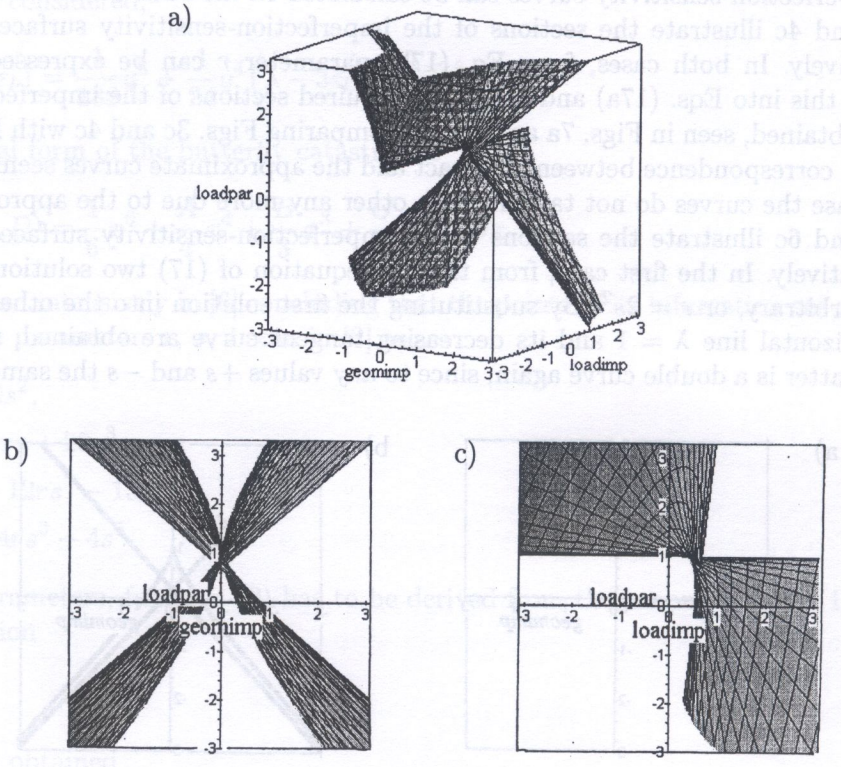

Fig. 9. Geometric-loading imperfection-sensitivity surface $\lambda_{cr}(\varepsilon_g\,,\,\varepsilon_l)$ of stable-symmetric bifurcation, representing butterfly catastrophe

5. Conclusion

Imperfection-sensitivity analysis was presented by comparing the classical and catastrophe theory methods in the case of the classical stable-symmetric bifurcation problem.

Generally, by using classical methods, no analytical solutions can be found for the imperfection-sensitivity functions, being multivalued representing the folded characteristics of the corresponding surfaces. In this paper, an approximate solution based on the catastrophe theory was introduced, by means of which, not only the sections but even the whole surface of imperfection-sensitivity could be obtained, in both numerical and graphical forms.

The analysis was based on the principle of the catastrophe theory, according to which, by considering the problem as an imperfect version of a higher order catastrophe, a topologically good solution can be obtained in a considerably large domain. The stable-symmetric bifurcation problem with geometric imperfection yields a *cusp* catastrophe. Thus, by introducing a new imperfection, namely, the deformation-dependence of the loading, the problem leads to the higher order *butterfly* catastrophe. The approximation through Taylor-expansion was applied to the butterfly catastrophe, to its canonical form, yielding a parametric description of the imperfection-sensitivity surfaces.

By comparing the classical and catastrophe theory methods in aspect of Taylor expansion, it can be stated that for the classical method the Taylor expansion in the critical point of the perfect structure provides a relatively good solution for a smaller domain. However, the catastrophe theory determines the point at which the Taylor expansion yields a good solution for a larger domain, too.

It is known that the catastrophe theory provides topologically exact *local* solutions. It was proved in this paper that by using the catastrophe theory, not only topologically exact results can be obtained, but, by applying a higher order catastrophe, considerable good solution can be obtained for a *quasi-global* domain, too. Moreover, the catastrophe theory solution provides the possibility of visualising the very complicated imperfection-sensitivity surfaces, too. This advantage stems from the parametric description of the canonical forms of the types of catastrophes. Thus, by using the catastrophe theory, the multivalued functions and the corresponding highly folded imperfection-sensitivity surfaces can be shown in a three dimensional representation.

The presented method has theoretical importance first. Indeed, to apply it for more dimensional problems yields difficulties. Nevertheless, it has been confirmed in this paper that the catastrophe theory can give helpful tools in imperfection-sensitivity analyses.

Acknowledgement

The study was supported by the National Development and Research Foundation (OTKA T025256)

References

[1] Z.P. Bazant, L. Cedolin. *Stability of Structures. Elastic, Inelastic, Fracture and Damage Theories.* Oxford University Press, New York, Oxford, 1991.

[2] Zs. Gáspár. Stability of elastic structures with the aid of the catastrophe theory. In: L. Kollár, ed., *Structural Stability in Engineering Practice.* E & FN SPON, London, 1999.

[3] M. Kurutz. Modification of the structural tangent stiffness due to nonlinear configuration-dependent conservative loading. *Computer Assisted Mechanics and Engineering Sciences*, **3**(4): 367–388. 1996.

[4] M. Kurutz. Postbifurcation equilibrium paths due to nonlinear configuration-dependent conservative loading by using nonsmooth analysis. *Journal of Mechanics of Structures and Machines*, **25**(4): 445–476. 1997.

[5] M. Kurutz. Imperfection-sensitivity of the classical bifurcation models loaded by configuration-dependent devices. *Journal of Mechanics of Structures and Machines*, **28**(1): 1–48, 2000.

[6] T. Poston, I.N. Stewart. *Catastrophe Theory and its Applications.* Pitman, London, 1978.

[7] J.M.T. Thompson, G.W. Hunt. *A General Theory of Elastic Stability.* Wiley, London, 1973.

[8] J.M.T. Thompson, G.W. Hunt. *Elastic Instability Phenomena.* Wiley, Chichester, 1984.